The fact that with the present analysis a combination of the metal radius and coordination number accounts for slightly less than half of the metal–ligand distance variability in tetravalent systems, whereas these factors can compensate for >80% of the variation in divalent and trivalent compounds, *might* be taken as an indication that covalent effects are introducing significant nonlinear deviations from the trends expected from an ionic bonding model. Just as reasonably, however, the poor correlation in tetravalent complexes may indicate that ligand–ligand contacts in the highly coordinated compounds are sufficiently complicated that a detailed analysis of steric interactions will be required for the interpretation of the geometries of these systems. Only then should covalency be introduced as an explanation for structural anomalies in such cyclopentadienyl complexes.

## Conclusions

Analysis of metal–cyclopentadienyl distances in a large number of alkaline-earth-element and f-element complexes makes it evident that a unique value for the cyclopentadienyl radius does not exist. Metal–Cp distances are a function of both the radius of the metal center and amount of ligand–ligand contact on the coordination sphere of the metal, which can be correlated with the oxidation state and, to a lesser extent, the coordination number of the metal center. The concept of an "effective ionic radius" for the Cp ligand is still useful in the case of divalent complexes, however, and can be used with certain classes of trivalent species if complexes with similar ligand sets are used as the basis for comparison. No consistent value for the Cp radius can be found for tetravalent cyclopentadienyl compounds.

A rigorous analysis of ligand–ligand repulsions is obviously of paramount importance for the prediction of structures of ionically bonded organometallic compounds. Attempts toward modeling these interactions in a quantitative fashion for both cyclopentadienyl systems and other ionic complexes are in progress.

**Acknowledgment** is made to the donors of the Petroleum Research Fund, administered by the American Chemical Society, for support of this research.

**Supplementary Material Available:** Tables of multiple regression coefficients for M–Ω and M–C distances vs metal radius, oxidation number, and coordination number and of regression coefficients for M–Ω and M–C distances vs metal radius for complexes divided by oxidation states and a complete listing of and literature references for all complexes used in this study (17 pages). Ordering information is given on any current masthead page.

---

Contribution from the Institute of Chemistry, Academia Sinica, Taipei, Taiwan, ROC

# Electron Delocalization in Mixed-Valence Biferrocenium Salts: Nuclear Magnetic Resonance Contact Shift Studies

Teng-Yuan Dong,* Ming-Yhu Hwang, Tsui-Ling Hsu, Chi-Chang Schei, and Show-Kei Yeh

*Received May 10, 1989*

1′,6′-Diethenylbiferrocenium triiodide (**6**) was prepared, and the intramolecular electron-transfer rate was determined. The X-ray structure of 1′,6′-diethenylbiferrocene at 300 K has been determined: monoclinic, $P2_1/n$, $a$ = 5.7977 (4) Å, $b$ = 17.2970 (20) Å, $c$ = 9.1994 (13) Å, and $\beta$ = 90.210 (15)°; $\rho_{calcd}$ = 1.520 g cm$^{-3}$, $Z$ = 2, $R_F$ = 0.04, and $R_{wF}$ = 0.03. The $^1$H and $^{13}$C NMR contact shifts have been observed for a series of mixed-valence biferrocenium triiodides. Analysis of the sign of contact shifts suggests that the electron delocalization is based on competing $\sigma$ and $\pi$ delocalization mechanisms. It appears that the $\sigma$ skeleton in the delocalization of spin density is strongly favored in the cyclopentadienyl moiety. The unpaired spin delocalization in $\pi$-type orbitals is found to predominate in the fulvenide moiety.

## Introduction

Discoveries made in the last few years have shown that the solid-state environment plays a crucial role in determining the rate of intramolecular electron transfer in various mixed-valence complexes.[1] In the case of binuclear mixed-valence biferrocenium compounds, it has been found that the nature of the solid-state environment about a mixed-valence cation can dramatically affect the rate of intramolecular electron transfer.[2-8] Several important observations have been made on the mixed-valence compounds **1**–**5**.[3,4,8] Compounds **2**–**5** give unusual temperature-dependent

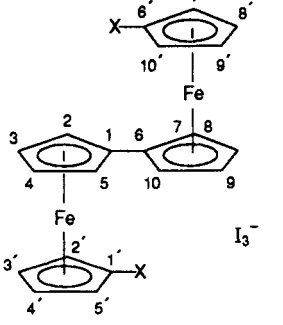


X = H (**1**), $C_2H_5$ (**2**), $C_3H_7$ (**3**), $C_4H_9$ (**4**), $CH_2C_6H_5$ (**5**), $CH{=}CH_2$ (**6**)

Mössbauer spectra. At temperatures below 200 K they each show two doublets, one for the $Fe^{II}$ and the other for the $Fe^{III}$ site. Increasing the sample temperature in each case causes the two doublets to move together with no discernible line broadening and eventually to become a single "average-valence" doublet at temperatures of 275, 245, 275, and 260 K, respectively. Furthermore, pronounced sample history dependencies of rates of electron transfer have been noted for compounds **1**, **4**, and **5**. For example, a microcrystalline sample of **5** gives a 300 K Mössbauer spectrum which is dominantly that of a valence-localized species (i.e., two

(1) Hendrickson, D. N.; Oh, S. M.; Dong, T.-Y.; Moore, M. F. *Comments Inorg. Chem.* **1985**, *4*(6), 329.
(2) Dong, T.-Y.; Cohn, M. J.; Hendrickson, D. N.; Pierpont, C. G. *J. Am. Chem. Soc.* **1985**, *107*, 4777.
(3) Cohn, M. J.; Dong, T.-Y.; Hendrickson, D. N.; Geib, S. J.; Rheingold, A. L. *J. Chem. Soc., Chem. Commun.* **1985**, 1095.
(4) (a) Dong, T.-Y.; Hendrickson, D. N.; Iwai, K.; Cohn, M. J.; Reingold, A. L.; Sano, H.; Motoyama, I.; Nakashima, S. *J. Am. Chem. Soc.* **1985**, *107*, 7996. (b) Konno, M.; Hyodo, S.; Iijima, S. *Bull. Chem. Soc. Jpn.* **1982**, *55*, 2327. (c) Nakashima, S.; Masuda, Y.; Motoyama, I.; Sano, H. *Bull. Chem. Soc. Jpn.* **1987**, *60*, 1673. (d) Nakashima, S.; Katada, M.; Motoyama, I.; Sano, H. *Bull. Chem. Soc. Jpn.* **1987**, *60*, 2253.
(5) (a) Dong, T.-Y.; Hendrickson, D. N.; Pierpont, C. G.; Moore, M. F. *J. Am. Chem. Soc.* **1986**, *108*, 963. (b) Motoyama, I.; Suto, K.; Katada, M.; Sano, H. *Chem. Lett.* **1983**, 1215. (c) Kai, M.; Motoyama, I.; Katada, M.; Masuda, Y.; Sano, H. *Chem. Lett.* **1988**, 1037.
(6) Dong, T.-Y.; Kambara, T.; Hendrickson, D. N. *J. Am. Chem. Soc.* **1986**, *108*, 4423.
(7) Dong, T.-Y.; Kambara, T.; Hendrickson, D. N. *J. Am. Chem. Soc.* **1986**, *108*, 5857.
(8) Sorai, M.; Nishimori, A.; Hendrickson, D. N.; Dong, T.-Y.; Cohn, M. J. *J. Am. Chem. Soc.* **1987**, *109*, 4266.

0020-1669/90/1329-0080$02.50/0 

doublets). However, a crystalline sample of **5** grown by diffusing hexane into a $CH_2Cl_2$ solution of **5** gives a Mössbauer spectrum with one average-valence doublet at 260 K. A detailed theoretical model[9] has been presented to show the effects of cooperative phase transition on the electronic delocalization in mixed-valence biferrocenium salts.

In extending our studies on intramolecular electron-transfer in mixed-valence biferrocenium salts, we report in this paper the preparation and characterization of the new compound **6**. A single-crystal X-ray structure is also reported for 1′,6′-diethenylbiferrocene. The application of NMR techniques to elucidate the nature of electron delocalization in the series of mixed-valence compounds is also presented.

## Experimental Section

**Compound Preparation.** Samples of ethenylferrocene,[10] biferrocene,[11] 1′,6′-dibutylbiferrocene,[4] 1′,6′-dibenzylbiferrocene,[12] and 1′,6′-diacetylbiferrocene[13] were prepared according to literature methods and identified by NMR and mass spectral data.

1′,6′-Diethenylbiferrocene was prepared by starting with 1′,6′-diacetylbiferrocene, which was reduced with $LiAlH_4$ to 1′,6′-bis(2-hydroxyethyl)biferrocene in ether solution. 1′,6′-Bis(2-hydroxyethyl)-biferrocene (0.52 g, 1.13 mmol) was dehydrated by using $CuSO_4$ (6.27 g, 39.15 mmol) catalyst in boiling toluene (100 mL) with hydroquinone (0.011 g, 0.1 mmol) inhibitor. The mixture was refluxed with stirring for 1 h. At the end of the reaction, the mixture was filtered, and the precipitate collected on a filter was washed several times with $CH_2Cl_2$. The filtrate and the washings were combined. After the removal of the solvent, the residual crude product was chromatographed on neutral alumina (activity I) with hexane to afford 0.23 g of 1′,6′-diethenylbiferrocene. The properties are as follows: $^1H$ NMR ($CDCl_3$) $\delta$ 3.8–4.3 (16 H, m), 4.92 (1.9 H, d), 5.18 (1.9 H, d), 6.25 (2 H, dd); electron-impact mass spectrum $m/e$ 422 ($M^+$).

Samples of 1′,6′-dibutylbiferrocenium triiodide (**4**), 1′,6′-dibenzylbiferrocenium triiodide (**5**), and 1′,6′-diethenylbiferrocenium triiodide (**6**) were prepared according to the simple procedure previously reported for biferrocenium triiodide.[14] Anal. Calcd for **4** ($C_{28}H_{34}Fe_2I_3$): C, 38.97; H, 3.97. Found: C, 38.81; H, 3.79. Calcd for **5** ($C_{34}H_{30}Fe_2I_3$): C, 43.86; H, 3.25. Found: C, 43.72; H, 3.37. Calcd for **6** ($C_{24}H_{22}Fe_2I_3$): C, 35.91; H, 2.76. Found: C, 36.17; H, 2.82.

**Physical Methods.** At the Academia Sinica $^{57}Fe$ Mössbauer measurements were made on a constant-acceleration-type instrument. The source, which originally consisted of 50 mCi of $^{57}Co$ diffused into a 12-$\mu$m rhodium matrix, is connected to a Ranger Scientific Model VT-700 velocity transducer. An Ortec Model 5600 multichannel analyzer, scanned over 1024 channels, receives the logic pulses from the single-channel analyzer. Computer fittings of the $^{57}Fe$ Mössbauer data to Lorentzian lines were carried out with a modified version of a previously reported program.[15] Velocity calibrations were made with use of a 99.99% pure 10-$\mu$m iron foil. Typical line widths for all three pairs of iron lines fell in the range of 0.28–0.32 mm/s. Isomer shifts are reported with respect to iron foil at 300 K.

$^1H$ and $^{13}C$ NMR spectra were run on a Bruker MSL 200 spectrometer. Mass spectra were obtained with a Hewlett-Packard Model 5995 GC/MS system. Near-IR spectra were recorded with a Perkin-Elmer Lambda 9 spectrophotometer in $CD_2Cl_2$ using 1.0-cm quartz cells from 2600 to 900 nm.

Polarographic measurements were carried out with a Princeton Applied Research Model 173 polarograph. Cyclic voltammetry was performed with a stationary Pt electrode, which was cleaned after each run. Duplicate runs were made on each sample. In most cases the polarographic measurements were run on $1 \times 10^{-3}$ M acetonitrile solutions with 0.1 M $(n\text{-}C_4H_9)_4NBF_4$ as supporting electrolyte. Degassing with nitrogen prefaced each run. The potentials quoted in this work are referred to a saturated aqueous calomel electrode at 25 °C.

**Table I.** Experimental and Crystal Data for the X-ray Structure of 1′,6′-Diethenylbiferrocene

| Crystal Parameters | |
|---|---|
| cryst syst: monoclinic | space group: $P2_1/n$ |
| $a$ = 5.7977 (4) Å | $\beta$ = 90.210 (15)° |
| $b$ = 17.2970 (20) Å | $Z$ = 2 |
| $c$ = 9.1994 (13) Å | $\mu$ = 1.58 mm$^{-1}$ |
| $V$ = 922.54 Å$^3$ | fw = 421.98 |
| $\rho_{calcd}$ = 1.520 g cm$^{-}$ | |

| Data Measurement |
|---|
| radiation: graphite-monochromatized Mo K$\alpha$ |
| $2\theta$ limits: $0.0° < 2\theta < 49.8°$ |
| for signif reflns: $R_F{}^a$ = 0.025; $R_{wF}{}^a$ = 0.028 |
| for all rflns: $R_F{}^a$ = 0.04; $R_{wF}{}^a$ = 0.030 |

$^a R_F = \sum||F_o| - |F_c||/\sum F_o$; $R_{wF} = [\sum w(F_o - |F_c|)^2/\sum wF_o^2]^{1/2}$.

**Table II.** Atom Coordinates and Thermal Factors

| atom | $x$ | $y$ | $z$ | $U_{iso}$,$^a$ Å$^2$ |
|---|---|---|---|---|
| Fe | 0.33464 (7) | 0.136743 (20) | 0.53022 (4) | 2.381 (17) |
| C1A | 0.4701 (5) | 0.02703 (14) | 0.5573 (3) | 2.24 (10) |
| C2A | 0.6153 (5) | 0.08375 (16) | 0.6217 (3) | 2.81 (12) |
| C3A | 0.4892 (6) | 0.12397 (18) | 0.7288 (3) | 3.52 (14) |
| C4A | 0.2643 (6) | 0.09341 (18) | 0.7312 (3) | 3.36 (13) |
| C5A | 0.2515 (5) | 0.03380 (16) | 0.6265 (3) | 2.66 (12) |
| C1B | 0.3020 (5) | 0.15927 (16) | 0.3117 (3) | 3.03 (12) |
| C2B | 0.0851 (5) | 0.16442 (17) | 0.3825 (3) | 2.99 (12) |
| C3B | 0.0989 (6) | 0.22187 (17) | 0.4915 (4) | 3.37 (13) |
| C4B | 0.3237 (6) | 0.25224 (18) | 0.4890 (4) | 3.92 (15) |
| C5B | 0.4484 (6) | 0.21404 (18) | 0.3792 (4) | 3.63 (14) |
| C1 | 0.3651 (8) | 0.10689 (22) | 0.1941 (4) | 4.43 (17) |
| C2 | 0.2255 (11) | 0.0629 (3) | 0.1203 (5) | 6.2 (3) |
| H2A | 0.759 (5) | 0.0922 (14) | 0.597 (3) | 1.9 (6) |
| H3A | 0.540 (5) | 0.1654 (16) | 0.785 (3) | 3.3 (6) |
| H4A | 0.154 (5) | 0.1106 (16) | 0.787 (3) | 3.0 (7) |
| H5A | 0.125 (4) | 0.0051 (14) | 0.604 (3) | 2.0 (6) |
| H2B | −0.042 (5) | 0.1358 (15) | 0.364 (3) | 2.8 (6) |
| H3B | −0.020 (5) | 0.2342 (16) | 0.556 (3) | 3.8 (7) |
| H4B | 0.381 (5) | 0.2892 (16) | 0.548 (3) | 3.4 (7) |
| H5B | 0.602 (5) | 0.2243 (7) | 0.356 (3) | 4.4 (8) |
| H1 | 0.518 (6) | 0.1038 (21) | 0.165 (4) | 5.2 (9) |
| H21 | 0.291 (7) | 0.0306 (24) | 0.054 (4) | 7.8 (12) |
| H22 | 0.060 (9) | 0.067 (3) | 0.145 (5) | 10.8 (18) |

$^a U_{iso}$ is the equivalent isotropic $U$ defined as one-third of the trace of the orthogonalized $U_{ij}$ tensor.

**X-ray Structure Solution and Refinement for 1′,6′-Diethenylbiferrocene.** An orange needle crystal (0.10 × 0.15 × 0.55 mm), which was grown by slow evaporation from an ether solution, was used for data collection at room temperature on an Enraf-Nonius CAD4 diffractometer using the $\theta/2\theta$ scan mode at the Academia Sinica. Details of data collection may be found in Table I. The cell constants, listed in Table I, were obtained by a least-squares fit to the automatically centered settings for 25 strong reflections. Absorption corrections were made.

The structure was solved by heavy-atom methods. All non-hydrogen atoms were refined anisotropically. The final positional parameters for all atoms can be found in Table II, and the selected bond distances and angles are given in Table III.

## Results and Discussion

**Molecular Structure of 1′,6′-Diethenylbiferrocene.** The results of our crystallographic analysis show that the molecule exists in a trans conformation with the two iron ions on opposite sides of the planar fulvenide ligand. A perspective drawing of the molecule is shown in Figure 1. Table III lists important bond distances and angles. The planes of the ethenylcyclopentadienyl ligands form a dihedral angle of 2.21° with the fulvenide plane; furthermore, the two rings are perfectly eclipsed within experimental error. The average bond distances from the iron atom to the five carbon atoms of a given ring are 2.048 (3) and 2.041 (3) Å for the fulvenide and ethenylcyclopentadienyl rings, respectively. These distances are closer to the value of 2.045 Å found for ferrocene[16] than the value of 2.075 Å found for the ferrocenium[17]

(9) Kambara, T.; Hendrickson, D. N.; Dong, T.-Y.; Cohn, M. J. *J. Chem. Phys.* **1987**, *86*, 2362.
(10) (a) Rausch, M. D.; Siegel, A. *J. Organomet. Chem.* **1968**, *11*, 317. (b) Lai, J. C.; Rounsfell, T.; Pittman, C. U., Jr. *J. Polym. Sci., Polym. Chem. Ed.* **1971**, 651.
(11) Rausch, M. D. *J. Org. Chem.* **1961**, *26*, 1802.
(12) Yamakawa, K.; Hisatome, M.; Sako, Y.; Ichida, S. *J. Organomet. Chem.* **1975**, *93*, 219.
(13) Nesmeyanov, A. N.; Drozd, V. N.; Sazonova, V. A.; Romanenko, V. I.; Prokofev, A. K.; Nikonova, L. A. Izv. *Akad. Nauk SSSR, Ser. Khim.* **1963**, 667.
(14) Morrison, W. H., Jr.; Hendrickson, D. N. *Inorg. Chem.* **1975**, *14*, 2331.
(15) Lee, J. F.; Lee, M. D.; Tseng, P. K. *Chemistry* (in Chinese) **1987**, *45*, 50.
(16) Seiler, P.; Dunitz, J. D. *Acta Crystallogr., Sect. B* **1979**, *35*, 1068.

**Table III.** Selected Bond Distances and Angles

| | | | |
|---|---|---|---|
| | Interatomic Distances (Å) | | |
| Fe–C1A | 2.0685 (24) | C4A–C5A | 1.413 (4) |
| Fe–C2A | 2.046 (3) | C1B–C2B | 1.421 (4) |
| Fe–C3A | 2.044 (3) | C1B–C5B | 1.414 (5) |
| Fe–C4A | 2.037 (3) | C1B–C1 | 1.459 (5) |
| Fe–C5A | 2.047 (3) | C2B–C3B | 1.413 (5) |
| Fe–C1B | 2.056 (3) | C3B–C4B | 1.405 (5) |
| Fe–C2B | 2.038 (3) | C4B–C5B | 1.409 (5) |
| Fe–C3B | 2.039 (3) | C1–C2 | 1.300 (7) |
| Fe–C4B | 2.034 (3) | C1A–C1A(a) | 1.452 (5) |
| Fe–C5B | 2.040 (3) | C1A–C2A | 1.421 (4) |
| C1A–C5A | 1.425 (4) | C2A–C3A | 1.412 (4) |
| C3A–C4A | 1.407 (5) | | |
| | Angles (deg) | | |
| C3A–C2A–H2A | 126.5 (16) | C2A–C1A–C5A | 106.48 (24) |
| C2A–C3A–C4A | 107.9 (3) | C1A(a)–C1A–C5A | 126.32 (24) |
| C3A–C4A–C5A | 108.0 (3) | C3B–C4B–C5B | 108.4 (3) |
| C1A–C5A–C4A | 108.7 (3) | C1B–C5B–C4B | 108.7 (3) |
| C2B–C1B–C5B | 106.7 (3) | C1B–C1–C2 | 126.4 (4) |
| C2B–C1B–C1 | 127.1 (3) | C1B–C1–H1 | 119.6 (21) |
| C5B–C1B–C1 | 126.2 (3) | C2–C1–H1 | 114.0 (21) |
| C1B–C2B–C3B | 108.7 (3) | C1–C2–H21 | 116 (3) |
| C2B–C3B–C4B | 107.5 (3) | C1–C2–H22 | 116 (3) |
| C1A(a)–C1A–C2A | 127.2 (3) | H21–C2–H22 | 127 (4) |
| C1A–C2A–C3A | 108.9 (3) | | |

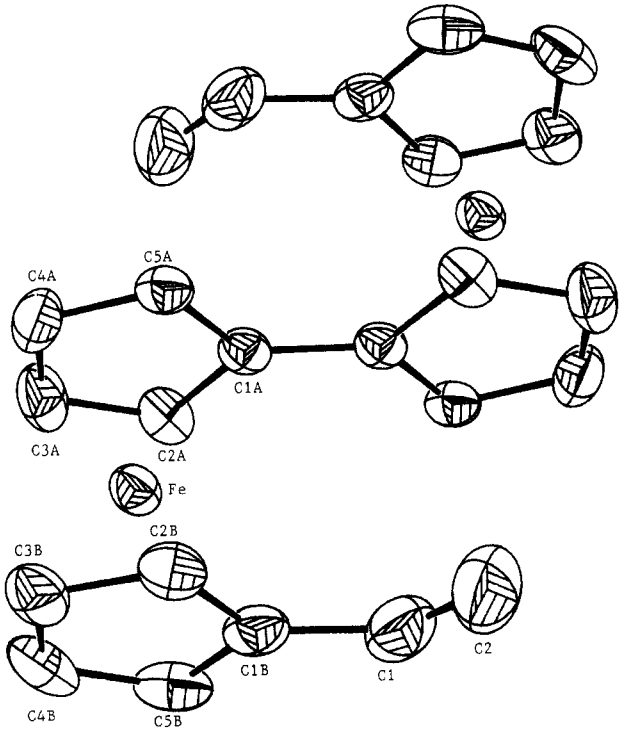


**Figure 1.** ORTEP plot of 1′,6′-diethenylbiferrocene with 50% probability thermal ellipsoids.

cation. The distance between centers of mass of the two rings is 3.307 Å. The planes of ethenyl substituents form a dihedral angle of 9.3° with the cyclopentadienyl planes. The average C–C bond length in the rings agrees well with those in ferrocene. The bond length and bond angles for ethenyl substituents are in good agreement with $sp^2$ hybridization. The distance between the two iron atoms is 5.136 Å.

**Electrochemical Results.** Table IV lists the polarographic data for 1′,6′-diethenylbiferrocene, as well as those for some other relevant biferrocenes. As shown in Table IV, it can be seen that in each biferrocene two oxidation waves are detected. Each wave corresponds to a one-electron process. The effect of substituents on the half-wave potential and the effects of ferrocene and ferrocenium groups as substituents have been shown to be additive.[18] In a general way, electron-donating groups stabilize the ferrocenium cation, lowering the half-wave potential, and electron-withdrawing groups have the opposite effect. From Table IV, biferrocene is more easily oxidized than ferrocene by 0.09 V. As a substituent, the ferrocenyl group clearly acts as a net electron donor and the ethenyl group acts as an electron-withdrawing group.

**Table IV.** Polarographic Data for Various Biferrocenes

| compd[a] | $E_{1/2}$, V | $\Delta$,[b] mV | $\Delta E_{1/2}$,[c] V |
|---|---|---|---|
| ferrocene | 0.40 | 65 | |
| ethenylferrocene | 0.42 | 70 | |
| biferrocene | 0.31 | 70 | 0.31 |
| | 0.62 | 75 | |
| 1′,6′-dibutylbiferrocene | 0.26 | 65 | 0.32 |
| | 0.58 | 65 | |
| 1′,6′-dibenzylbiferrocene | 0.31 | 70 | 0.32 |
| | 0.63 | 70 | |
| 1′,6′-diethenylbiferrocene | 0.31 | 75 | 0.33 |
| | 0.64 | 75 | |
| 1′,6′-diethenylbiferrocene[d] | 0.39 | 80 | 0.28 |
| | 0.67 | 80 | |

[a] All half-wave potentials are referred to the SCE, with use of a stationary Pt electrode. Measurements were run in $CH_3CN$ solutions unless stated otherwise. [b] Peak-to-peak separation between the resolved reduction and oxidation wave maxima. [c] Peak separation between waves. [d] Measurements were run in acetone solution.

**Table V.** $^{57}$Fe Mössbauer Least-Squares Fitting Parameters at 300 K

| compd | $\Delta E_Q$, mm/s | $\delta$, mm/s | $\Gamma$,[a] mm/s | |
|---|---|---|---|---|
| 1′,6′-diethenylbiferrocene | 2.235 | 0.446 | 0.250 | 0.249 |
| **1** | 1.907 | 0.452 | 0.268 | 0.260 |
| | 0.385 | 0.452 | 0.290 | 0.286 |
| **6** | 1.565 | 0.448 | 0.440 | 0.430 |
| | 0.706 | 0.441 | 0.422 | 0.425 |

[a] Full width at half-height taken from the least-squares fitting program. The width for the line at more negative velocity is listed first for each doublet.

It has been shown that the peak-to-peak separation ($\Delta E_{1/2}$) can gauge the interaction between two Fe sites.[19] A comparison of the magnitudes of $\Delta E_{1/2}$ in acetonitrile solution for the series of biferrocenes indicates that the interaction between the two Fe sites is probably not changing very much throughout the series. Furthermore, the smaller $\Delta E_{1/2}$ value of 1′,6′-diethenylbiferrocene in acetone solution could be explained by the known solvent effect. The effect of the reorganization of the solvent environment on the electron-transfer process for the two oxidation waves in 1′,6′-diethenylbiferrocene is different. It is interesting to note that the second oxidation wave is associated with an intramolecular electron-transfer process in monooxidized biferrocene. Monooxidized biferrocene is a class II mixed-valence compound. The solvent dependence of electron transfer for class II mixed-valence compounds has been investigated. The effect of solvent on intramolecular electron transfer in mixed-valence biferrocenium cations could be significant, and it is understandable why the different solvent effects for the two oxidation waves and a smaller $\Delta E_{1/2}$ value are being observed.

**$^{57}$Fe Mössbauer Characteristics.** Mössbauer spectroscopy is a particularly useful technique for probing the electronic states of iron ions in mixed-valence biferrocenium salts. Ferrocenyl groups give spectra characterized by large quadrupole splittings ($\Delta E_Q$) in the range of 2.0–2.5 mm/s, while the spectra of the ferrocenium cations are characterized by small or vanishing quadrupole splitting.

(17) Mammano, N. J.; Zalkin, A.; Landers, A.; Rheingold, A. L. *Inorg. Chem.* **1977**, *16*, 297.

(18) (a) Perevalova, E. G.; Gubin, E. O.; Smirnova, S. A.; Nesmeyanov, A. N. *Dokl. Akad. Nauk SSSR* **1964**, *155*, 857. (b) Kuwana, T.; Bublitz, D. E.; Hoh, G. *J. Am. Chem. Soc.* **1960**, *82*, 5811.

(19) Morrison, W. H., Jr.; Krogsrud, S.; Hendrickson, D. N. *Inorg. Chem.* **1973**, *12*, 1998.

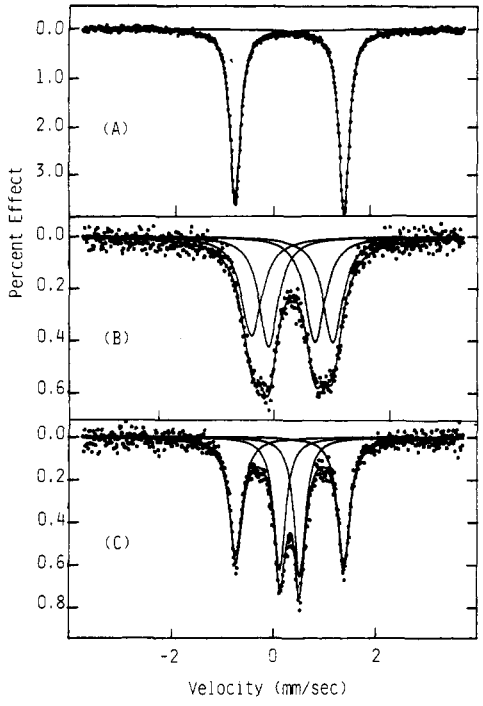


**Figure 2.** $^{57}$Fe Mössbauer spectra at 300 K for (A) 1′,6′-diethenylbiferrocene, (B) 1′,6′-diethenylbiferrocenium triiodide (**6**), and (C) biferrocenium triiodide (**1**).

Mössbauer spectra were run at 300 K for **6** and 1′,6′-diethenylbiferrocene (Figure 2). The various absorption peaks in each spectrum were least-squares fit to Lorentzian lines, and the resulting fitting parameters are summarized in Table V. The 300 K spectrum for **6** shows two doublets, one with a quadrupole splitting ($\Delta E_Q$) of 1.565 mm/s and the other with $\Delta E_Q$ = 0.706 mm/s. Both doublets have the same area. This pattern of two doublets is what is expected for a mixed-valence biferrocenium salt that is valence-trapped on the time scale of the Mössbauer technique. The thermal electron-transfer rate is less than $\sim 10^7$ $s^{-1}$.

Mössbauer spectra were also obtained for neutral 1′,6′-diethenylbiferrocene. The unoxidized compound gives a single doublet with $\Delta E_Q$ = 2.235 mm/s at 300 K. Thus, the $\Delta E_Q$ value of the ferrocenyl doublet for the mixed-valence compound is smaller than that for the unoxidized compound. We believe that the decrease of $\Delta E_Q$ in the ferrocenyl doublet and the increase of $\Delta E_Q$ in the ferrocenium doublet are related to the degree of intramolecular electron transfer in mixed-valence biferrocenium cations. As illustrated in Figure 2, a Mössbauer spectrum was also run at 300 K for compound **1**. Fitting parameters are given in Table V. The features in this spectrum are two doublets, one with $\Delta E_Q$ = 1.907 mm/s and the other with $\Delta E_Q$ = 0.385 mm/s. In the case of compound **6**, the behavior is different from what is seen for **1**. The two doublets in the 300 K spectrum of **6** just move together. Unfortunately, compound **6** decomposes at elevated temperatures. The conclusion from a comparison of the 300 K Mössbauer spectra of **1** and **6** is that the intramolecular electron transfer in **6** is faster than that in **1**.

**Infrared Spectroscopy.** IR spectroscopy has proven to be useful to tell whether or not a given mixed-valence biferrocenium cation is delocalized. It has been shown that the perpendicular C—H bending band is most diagnostic of the oxidation state.[20] This band is seen at 815 $cm^{-1}$ for ferrocene and at 851 $cm^{-1}$ for ferrocenium triiodide. Mixed-valence biferrocenium cations that have a non-negligible potential energy barrier for electron transfer should exhibit one C—H bending band for the $Fe^{II}$ moiety and one for the $Fe^{III}$ moiety. In the case of the new mixed-valence compound **6**, it will be interesting to see whether or not the C=C stretching mode is also useful in making a similar assessment.

(20) Kramer, J. A.; Hendrickson, D. N. *Inorg. Chem.* **1980**, *19*, 3330.

Infrared spectra were run for KBr pellets of 1′,6′-diethenylbiferrocene and **6**. In the perpendicular C—H bending region there is a strong band at 813 $cm^{-1}$ for unoxidized 1′,6′-diethenylbiferrocene. The mixed-valence compound **6** shows two C—H bending bands at 819 and 837 $cm^{-1}$, one for the $Fe^{II}$ moiety and one for the $Fe^{III}$ moiety as established for several mixed-valence biferrocenium cations.[4] However, the C=C stretching band observed at 1629 $cm^{-1}$ for unoxidized 1′,6′-diethenylbiferrocene is not detectable in the mixed-valence compound **6**.

**Near-Infrared Spectra.** In common with most mixed-valence complexes, the mixed-valence complex of **6** has a near-IR transition at 2100 nm that is not present for the neutral or dioxidized ion. The bandwidth ($\Delta\nu_{1/2}$, $\epsilon$ = 2200 $M^{-1}$ $cm^{-1}$ in $CD_2Cl_2$) at half-height is 15% sharper than what is expected on the basis of the equation given by Hush ($\Delta\nu_{1/2} = 2.82 \times 10^3$ $cm^{-1}$ compared to a calculated value of $3.32 \times 10^3$ $cm^{-1}$).[21] An agreement, to about 10%, between $\Delta\nu_{1/2}$(cal) and $\Delta\nu_{1/2}$(obs) is usually taken as an indication that the Hush model is a satisfactory description of a mixed-valence system.

The intensity of an intervalence transition band is dependent on the extent of interaction of the donor and acceptor sites in the ground state. The values of the interaction parameter ($\alpha$) and the electron-transfer rate constant ($K_{et}$) can be estimated from eq 1 and 2, respectively. In eq 1 and 2, the term $\epsilon_{max}$ is the

$$\alpha^2 \simeq (4.24 \times 10^{-4})[\Delta\nu_{1/2}]\epsilon_{max}/\bar{\nu}r^2 \quad (1)$$

$$K_{et} = (2\pi/\hbar)V_{ab}^2(\pi/K_B T\bar{\nu})^{1/2} \exp(-\bar{\nu}/4K_B T) \quad (2)$$

$$V_{ab} = [(4.24 \times 10^{-4})\epsilon_{max}(\Delta\nu_{1/2})\bar{\nu}/r^2]^{1/2} \quad (3)$$

extinction coefficient, $r$ is the donor–acceptor distance, $\alpha$ is the mixing coefficient, $\Delta\nu_{1/2}$ is the bandwidth, and $\bar{\nu}$ is the frequency. The average value of 5.1 Å in compounds **1**, **3**, **4**, and **5** is used as the donor–acceptor distance. Thus, $\alpha^2$ = 0.02 and $K_{et} = 5.14 \times 10^8$.

The energy and line shape of the IT band clearly indicate that the intramolecular electron-transfer rate of **6** in solution is greater than that of **6** in the solid state. In the past it has generally been assumed that the rate of intramolecular electron transfer in the solid state is similar to that in solution. The effect of the environment about the mixed-valence cation on the solid-state electron-transfer rate has been described.[2-8] In solution, the manner in which the mixed-valence cation is solvated also influences the rate of intramolecular electron transfer. For **6** in solution, we believe that the solvent molecules solvating the mixed-valence cation can adjust rapidly so that the electron-transfer rate is not limited.

**Nuclear Magnetic Resonance.** It is now widely recognized that the study of nuclear resonance in paramagnetic complexes can yield detailed information concerning metal–ligand bonding and electron delocalization. It is of value to apply the NMR technique to elucidate the nature of electron delocalization in the series of mixed-valence biferrocenium salts.

The $^1H$ and $^{13}C$ NMR spectra were obtained from saturated deoxygenated $CD_2Cl_2$ solutions. The contact shifts for the molecules of interest will be found in Table VI. Shifts were taken relative to the TMS peak. The contact shifts were calculated relative to the shifts for the corresponding biferrocenes. A comparison of the sign of the –CH= contact shift with that of the cyclopentadienyl proton contact shift in compound **6** leads to the conclusion that the unpaired electron density is delocalized in $\sigma$ (in-plane) cyclopentadienyl orbitals, not $\pi$-type orbitals as found in ferrocenium salts.[22-24] The $\pi$-polarization effect in metallocenes was first discussed by Levy and Orgel in 1960. It was considered that the unpaired $\pi$ electron in the cyclopentadienyl orbitals

(21) Hush, N. S. *Prog. Inorg. Chem.* **1967**, *8*, 391.
(22) Rettig, M. F.; Drago, R. S. *J. Am. Chem. Soc.* **1969**, *91*, 1361.
(23) Materikova, R. B.; Babin, V. N.; Solodovnikov, S. P.; Lyatifov, I. R.; Petrovsky, P. V.; Fedin, E. I. *Z. Naturforsch., B: Anorg. Chem., Org. Chem.* **1980**, *35B*(11), 1415.
(24) Kurbanov, T. Kh. *Azerb. Khim. Zh.* **1981**, *6*, 104.

**Table VI.** $^1$H NMR Data for Paramagnetic Mixed-Valence Biferrocenes at 298 K

| compd | exptl shifts[a] δ, ppm | line width, Hz | Δδ,[b] ppm |
|---|---|---|---|
| $(C_5H_5)_2FeI_3$[c] | 31.9 | 620 | 27.86 |
| **1**[d] | 17.78 (1 H, Cp) | 260 | |
| | 20.65 (8 H, fulvenide) | 320 | |
| **4**[e] | 1.78 (t, 5.9 H, δ-$CH_3$) | 8 | 0.90 |
| | 2.01 (m, 4 H, γ-$CH_2$) | 10 | 0.76 |
| | 3.52 (m, 4 H, β-$CH_2$) | 8 | 2.12 |
| | 15.25 (4 H, α-$CH_2$) | 90 | 13.08 |
| | 16.38 (overlap, ~4 H, fulvenide) | br | 12.22 |
| | 20.24 (overlap, ~4 H, fulvenide) | br | 15.94 |
| | 21.65 (overlap, ~8 H, Cp) | br | 17.78 |
| **5**[f] | 6.91 (4 H, $-CH_2$) | 70 | 3.53 |
| | 8.26 (9.3 H, $-CH_5$) | 10 | ~1.1 |
| | 16.47 (4 H, Cp) | 290 | |
| | 20.77 (12 H, Cp + fulvenide) | 350 | |
| **6**[d] | −3.90 (2 H, $=CH_2$) | 35 | −8.82 |
| | −2.73 (2 H, $=CH_2$) | 25 | −7.91 |
| | 11.32 (2 H, $-CH=$) | 60 | 5.07 |
| | 14.13 (4 H, fulvenide) | 260 | ~10 |
| | 19.81 (overlap, ~8 H, Cp) | br | ~15 |
| | 20.12 (overlap, ~4 H, fulvenide) | br | ~16 |
| **6**[g] | −0.40 (2 H, $=CH_2$) | 30 | −5.32 |
| | +0.44 (2 H, $=CH_2$) | 20 | −4.74 |
| | 9.54 (2 H, $-CH=$) | 50 | 3.29 |
| | 13.8 (4 H, fulvenide) | br | ~9 |
| | 15.0 (~8 H, Cp) | br | ~11 |
| | 17.3 (~4 H, fulvenide) | br | ~13 |

[a] Shifts were taken relative to the TMS peak. [b] Contact shifts were calculated relative to the shift for the corresponding diamagnetic biferrocene. [c] $^1$H NMR spectrum of ferrocene: δ 4.04 in $CD_2Cl_2$. [d] In $CD_2Cl_2$. [e] $^1$H NMR spectrum of 1′,6′-dibutylbiferrocene ($CD_2Cl_2$): δ 0.88 (6 H, δ-$CH_3$), 1.25 (4 H, γ-$CH_2$), 1.40 (4 H, β-$CH_2$), 2.17 (4 H, α-$CH_2$), 3.87 (8 H, Cp), 4.16 (4 H, fulvenide), 4.30 (4 H, fulvenide). [f] $^1$H NMR spectrum of 1′,6′-dibenzylbiferrocene ($CD_2Cl_2$): δ 3.38 (4 H, $-CH_2$), 3.87, 4.12, 4.25 (16 H, Cp + fulvenide), 7.0–7.3 (10 H, $-C_6H_5$). [g] In $CD_3CN$ solution.

polarizes the C–H σ bond. This would lead to negative spin density and positive contact shifts at the protons in metallocenes. Retting,[22] Materikova,[23] and Kurbanov[24] reported the $^1$H and $^{13}$C NMR spectra for ferrocenium and 1,1′-dimethylferrocenium ions. For the 1,1′-dimethylferrocenium cation, the negative spin density at cyclopentadienyl protons and the positive spin density at methyl protons led the authors to propose the π-skeleton spin delocalization. However, in the case of the decamethylferrocenium salt Kurbanov[24] found the σ skeleton has a more important role. The general pattern of the spin delocalization for metallocene depends on the superposition of the π and σ mechanisms. In the $^1$H NMR spectra of **6**, the negative spin density at cyclopentadienyl protons and the vinyl proton suggests strongly that the unpaired spin density is in fact in cyclopentadienyl σ orbitals rather than π orbitals. Electron delocalization in ligand σ orbitals has been observed for 1,1′-dimethylchromocene[22] and nickel complexes of pyridine[25] and aliphatic amines.[26] It should be pointed out that the π mechanism plays a leading role in delocalization of spin density in the ethenyl substituents. The two upfield-shifted lines

(25) Happe, J.; Ward, R. L. *J. Chem. Phys.* **1963**, *39*, 1211.
(26) Fitzgerald, R. J.; Drago, R. S. *J. Am. Chem. Soc.* **1968**, *90*, 2523.

**Table VII.** $^{13}$C NMR Data for **4** in $CD_2Cl_2$

| exptl shift[a] δ, ppm | line width, Hz | Δδ,[b] ppm |
|---|---|---|
| −8.61 ($C_{2,5,7,10}$ or $C_{3,4,8,9}$) | 30 | negative |
| 2.32 ($C_{2,5,7,10}$ or $C_{3,4,8,9}$) | 8 | negative |
| 15.54 (δ-C) | 2 | 1.62 |
| 22.97 (γ-C) | 2 | 0.12 |
| 48.52 (β-C) | 6 | 19.90 |
| 113.68 (α-C) | 12 | 80.27 |
| 140.25 ($C_{2',5',7',10'}$ or $C_{3',4',8',9'}$) | 12 | positive |
| 168.84 ($C_{2',5',7',10'}$ or $C_{3',4',8',9'}$) | 12 | positive |

[a] Shifts were taken relative to the TMS peak. The carbons that are labeled 1, 1′, 6, and 6′ are not detectable. [b] $^{13}$C NMR spectrum of 1′,6′-di-*n*-butylbiferrocene: δ 13.92 (δ-C), 22.85 (γ-C), 28.62 (β-C), 33.41 (α-C), 66.63 ($C_{2,5,6,7}$) or $C_{3,4,8,9}$), 68.41 ($C_{2',3',4',5',7',8',9',10'}$), 69.41 ($C_{2,5,6,7}$ or $C_{3,4,8,9}$), 84.91 ($C_{1',6'}$), 90.41 ($C_{1,6}$).

at −2.73 and −3.89 ppm must be assigned to the vinylidene protons on the basis of intensity measurements and the sign of contact shifts. The delocalization of unpaired electron density in σ cyclopentadienyl orbitals of mixed-valence compound **4** is also observed. For *n*-butyl attached to the ring, the experimentally observed $^1$H NMR contact shifts are as follows: α-$CH_2$, +13.08 ppm; β-$CH_2$, +2.13 ppm; γ-$CH_2$, +0.76 ppm; δ-$CH_2$, +0.91 ppm. The cyclopentadienyl protons also have a downfield shift (+17.78 ppm). The assignments of peaks for compound **4** are based on intensity measurements and line widths.

One may wonder about whether or not the σ skeleton still plays a leading role in the fulvenide moiety. Fortunately, the high solubility of compound **4** allows us to apply the $^{13}$C NMR technique to establish the argument. The $^{13}$C NMR data of **4** are listed in Table VII. The $^{13}$C NMR contact shifts are as follows: α-C, +80.27 ppm; β-C, +19.89 ppm; γ-C, +0.13 ppm; δ-C, +1.61 ppm. The assignments are based on line widths and the requirement of positive $^{13}$C NMR contact shifts. The two downfield-shifted lines at 140.25 and 168.84 ppm are assigned to the cyclopentadienyl carbons on the basis of line widths and the requirement of positive $^{13}$C NMR contact shifts. The remaining two upfield-shifted lines at −8.61 and 2.32 ppm must be assigned to the fulvenide carbons. The negative spin density at protons and positive spin density at carbons indicate the π-mechanism becomes dominant in the fulvenide moiety. The observed contact shifts in compounds **4** and **6** suggest that the nature of electron delocalization involves a competition of σ and π delocalization mechanisms. Furthermore, the spin density and the competition of σ and π mechanisms are different from one cation to another. In the $^1$H NMR studies, we do observe that the contact shifts are different from one cation to another in the series of mixed-valence biferrocenium salts. In the case of **6**, the contact shifts can be varied by changing the solvent from $CD_2Cl_2$ to $CD_3CN$. It is likely that the change of contact shifts reflects the degree of delocalization in the mixed-valence cations.

**Acknowledgment.** We are grateful for support from the National Science Council (Grant No. NSC-77-0208-M001-01).

**Registry No.** **1**, 39470-17-2; **4**, 96898-15-6; **5**, 96898-17-8; **6**, 124021-20-1; ferrocene, 102-54-5; ethenylferrocene, 1271-51-8; biferrocene, 1287-38-3; 1′,6′-dibutylbiferrocene, 1298-95-9; 1′,6′-dibenzylbiferrocene, 56770-50-4; 1′,6′-diethenylbiferrocene, 124021-18-7; 1′,6′-diacetylbiferrocene, 12203-92-8; 1′,6′-bis(2-hydroxyethyl)biferrocene, 124021-21-2.

**Supplementary Material Available:** A table of anisotropic thermal parameters (1 page); a table of observed and calculated structure factors (12 pages). Ordering information is given on any current masthead page.